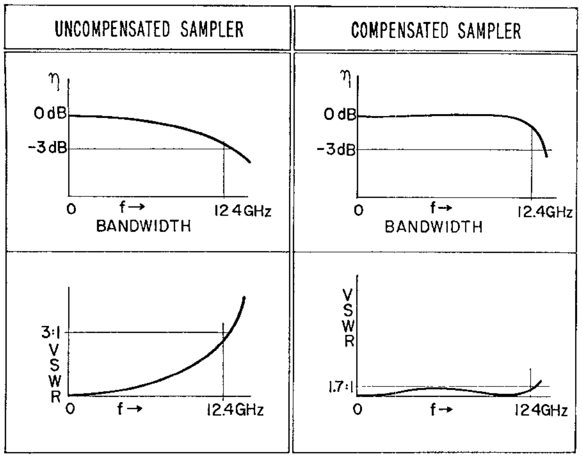

Fig. 15. Average measured performance.

Conclusion

The bandwidths obtained, using the electromechanical configuration just described, are well in excess of 12.4 GHz. This represents an increase in bandwidth of three to four times that previously available. It is safe to assume that this technique will eventually be used to achieve bandwidths in excess of 18 GHz.

Acknowledgment

The author wishes to acknowledge the helpful suggestions of Dr. B. Oliver, Vice President of Research at the Hewlett-Packard Company, and the devoted work of the many individuals at -hp- Associates, who contributed to the development work described here.

References

[1] R. Sugarman, "Sampling oscilloscope for statistically varying pulses," *Rev. Sci. Instr.*, vol. 28, pp. 933–938, November 1957.
[2] J. M. L. Janssen, "An experimental 'stroboscopic' oscilloscope for frequencies up to about 50 mc/s," *Phillips Tech. Rev.*, vol. 12, pp. 52–58, 1950 and vol. 12, pp. 73–81, September 1950.
[3] E. Hospitalier, "The slow registration of rapid phenomena by strobographic methods," *The Elec. Engr.* (*Melbourne, Australia*), pp. 40–44, January 1, 1904.
[4] G. B. B. Chaplin "A method of designing transistor avalanche circuits with application to a sensitive transitor oscilloscope," *Digest of Tech. Papers, IRE-AIEE 1958 Transistor and Solid-State Circuits Conf.*, pp. 21–23.
[5] H. L. Callendar, "An alternating cycle-curve recorder," *The Electrician*, pp. 582–586, August 26, 1898.
[6] E. W. Golding, *Electrical Measurements and Measuring Instruments*, 3rd ed., revised. London: Pitman and Sons, 1942.
[7] R. J. D. Reeves, "The recording and Collocation of Waveforms," *Electronic Engrg.*, vol. 31, pp. 130–137, March 1959 and vol. 31, pp. 204–212, April 1959.
[8] J. G. McQueen, "The monitoring of high-speed waveforms," *Electronic Engrg.*, pp. 436–441, October 1952.
[9] F. A. Laws, *Electrical Measurements*, 2nd ed. New York: McGraw-Hill, 1938.
[10] R. Carlson et al., "Sampling oscillography," *IRE WESCON Rec.*, pt. 8, pp. 44–51, 1959.
[11] R. Carlson, "A versatile new DC-500 MC oscilloscope with high sensitivity and dual channel display," *Hewlett-Packard J.*, vol. 11, nos. 5–7, January/March 1960.
[12] G. Frye and N. Nahman, "Random sampling oscillography," *IEEE Trans. on Instrumentation and Measurement*, vol. IM-13, pp. 8–13, March 1964.
[13] C. Yen, "Phase-locked sampling instruments," *IEEE Trans. on Instrumentation and Measurement*, vol. IM-14, pp. 64–68, March/June 1965.
[14] W. Grove, "A new DC-400 MC sampling 'scope plug-in with signal feed-through capability," *Hewlett-Packard J.*, vol. 15, no. 8, pp. 5–8, April 1964.
[15] H. Wallman and G. E. Valley, Jr., *Vacuum Tube Amplifiers*. New York: McGraw-Hill, 1948.
[16] J. Truxal, *Control Systems Synthesis*. New York: McGraw-Hill, 1955, pp. 36–40.
[17] S. A. Schelkunoff, *Advanced Antenna Theory*. New York: Wiley, 1952.

Theoretical and Practical Applications of Capacitance Matrix Transformations to TEM Network Design

R. J. WENZEL, MEMBER, IEEE

***Abstract*—TEM propagation on an array of parallel conductors is described in terms of the normalized static capacitance matrix. Important properties of capacitance matrices are discussed and a physical and network interpretation is given to a useful linear transformation of the static capacitance matrix. Several practical applications of capacitance matrix transformations are given. These include 1) equivalent circuits for directional couplers with equal terminations, 2) design procedures for directional couplers with unequal terminations, and 3) element value tables and design details for compact coaxial filter-transformers. Construction details and experimental results are presented for a 3:1 bandwidth filter-transformer constructed with multiple re-entrant coaxial lines.**

Manuscript received June 17, 1966; revised August 2, 1966. This work was supported by the U. S. Army Electronics Laboratory, Fort Monmouth, N. J., under Contracts DA 28-043 AMC-00399(E) and DA 28-043 AMC-01869(E).
The author is with The Bendix Corporation, Research Laboratories Division, Southfield, Mich.

I. Introduction

An important aspect of TEM quarter-wave network synthesis and design is the multiplicity of physical configurations that yield identical response characteristics. Different network configurations are often required to realize a desired response for moderate changes in design parameters because of the small range of realizable impedance values. In most design procedures (either exact or approximate), practical circuit element values are obtained by application of suitable equivalent circuit relationships.

In a previous paper [1], the concept of obtaining invariant transmission characteristics using transformations of the static capacitance matrix of a parallel-coupled line array was introduced and was applied to the exact design of interdigital bandpass filters. The purpose of this paper is to demonstrate in more detail the importance of the static capacitance matrix, to show how numerous equivalent circuits can be derived by its transformation, and to give a simple network and physical interpretation to the transformation.

The body of this paper is presented in Sections II and III. In Section II-A, the description of TEM transmission on an array of parallel conductors is given in terms of the static capacitance matrix and some basic properties of capacitance matrices are described and related to specific network geometries. In Section II-B, the capacitance matrix transformation is defined and a network and physical interpretation of this transformation is presented.

The application of the capacitance matrix transformation to the design of directional couplers with equal or unequal terminations is presented in Sections III-A and III-B. Element value tables and design information relative to the construction of compact filter-transformers based on the interdigital filter prototype are presented in Section III-C. Measured performance characteristics for an experimental 3:1 bandwidth filter-transformer are also given.

II. TEM Mode Coupled Line Theory and the Capacitance Matrix Transformation

A. The Static Capacitance Matrix C

TEM propagation on an array of $N+1$ parallel conductors can be described in terms of an $N \times N$ static capacitance matrix by consideration of the $2N$ coupled partial differential equations that apply to such a system. This problem has been considered by several authors [2]–[4] and it is readily shown that the $2N$-port voltages and currents defined in Fig. 1 are related by the admittance matrix $\boldsymbol{Y}$ as follows:

$$\left[\begin{array}{c} I_A \\ \hline I_B \end{array}\right] = \frac{1}{\eta_0 S}\left[\begin{array}{c|c} \boldsymbol{C} & -\boldsymbol{C}\sqrt{1-S^2} \\ \hline -\boldsymbol{C}\sqrt{1-S^2} & \boldsymbol{C} \end{array}\right] \cdot \left[\begin{array}{c} V_A \\ \hline V_B \end{array}\right] \qquad (1)$$

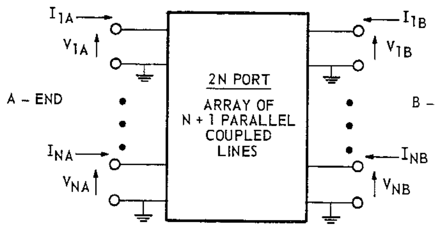

Fig. 1. $2N$-port network with admittance matrix $\boldsymbol{Y}$.

where

$\boldsymbol{C} = N \times N$ normalized static capacitance matrix with elements c,

$c = c'/\epsilon =$ ratio of the static capacitance between conductors per unit length to the permittivity of the medium (this ratio is independent of the dielectric medium and depends only on cross-section geometry). This dimensionless ratio is convenient for practical use with available design data [5], [6].

$\eta_0 = 376.6$ ohms, the impedance of free space,

$S = j \tan\theta$

$\theta = \pi\omega/2\omega_0 =$ electrical length of the lines in radians,

and

$\omega_0 =$ the frequency for which the lines are a quarter wavelength.

Other network matrices ($\boldsymbol{Z}$, $\boldsymbol{ABCD}$, $\boldsymbol{S}$, etc.) can be obtained by well-known transformations of (1) (see Reference [7]).

Some general properties of capacitance matrices will be discussed by considering the arbitrary array of four conductors shown in Fig. 2(a). Conductor 4 is taken as reference (ground). The 3 by 3 capacitance matrix has main diagonal terms given by the sum of all capacitors connected to each of the three ungrounded conductors and off-diagonal terms given by the negative of the capacitors between conductors. Therefore

$$\boldsymbol{C} = \left[\begin{array}{c|c|c} c_1 + c_{12} + c_{13} & -c_{12} & -c_{13} \\ \hline -c_{12} & c_2 + c_{12} + c_{23} & -c_{23} \\ \hline -c_{13} & -c_{23} & c_3 + c_{13} + c_{23} \end{array}\right]. \qquad (2)$$

The elements of matrix (2) satisfy the following relationships [8], [9]:

$$\begin{array}{lll} \text{a)} \displaystyle\sum_{k=1}^{N} c_{ik} \geq 0 & i = 1, 2, \cdots, N & \\ \text{b)}\ c_{ik} = c_{ki} & i \neq k & \\ \text{c)}\ c_{ii} \geq 0 & & \\ \text{d)}\ c_{ik} \leq 0 & i \neq k. & (3) \end{array}$$

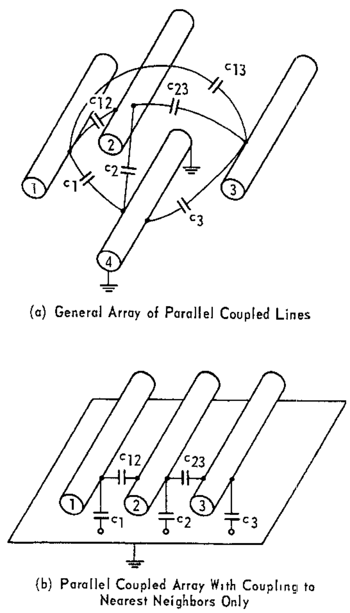

Fig. 2. Static capacitances of parallel coupled line arrays.

To obtain a physical realization for a network of the type shown in Fig. 2(a), starting from a given matrix $\boldsymbol{C}$, requires that physical dimensions be determined either experimentally or analytically by solution of Laplace's equation. Unfortunately, this is an extremely difficult problem, for most geometric configurations and solutions are known only for a few special cases. One case of particular interest is obtained by assuming that each conductor is coupled directly only to its nearest neighbors. This configuration is shown in Fig. 2(b), where conductor 4 is assumed to be a ground plane. The capacitance matrix for this network is given by

$$\boldsymbol{C} = \left[\begin{array}{c|c|c} c_1 + c_{12} & -c_{12} & 0 \\ \hline -c_{12} & c_{12} + c_2 + c_{23} & -c_{23} \\ \hline 0 & -c_{23} & c_3 + c_{23} \end{array}\right]. \tag{4}$$

The $\boldsymbol{C}$ matrix for a like array with any number of conductors is obtained in a similar manner. Note that the assumption of coupling only to nearest neighbors results in a matrix with nonzero elements on the main diagonal and adjacent to the main diagonal only. Given a $\boldsymbol{C}$ matrix of the above type, data exist from which physical dimensions can be determined [5], [6]. It is emphasized that the assumption of coupling to nearest neighbors only is not necessarily desirable from the viewpoint of obtaining optimum device performance from a given number of lines. Many useful devices might result if simple solutions to Laplace's equation were known for a larger number of geometries. On the other hand, networks with lines coupled only to nearest neighbors can realize a wide class of network functions and allow considerable versatility of cross-section geometry, as will be shown in succeeding sections. Throughout the remainder of the paper, only network geometries with lines directly coupled to nearest neighbors will be considered.

B. The Capacitance Matrix Transformation[1]

Different network configurations that leave some specified network response invariant are said to be "equivalent." A method of investigating possible equivalent circuits is to use a linear transformation of network variables (voltage and/or current, for example). Linear transformations of network variables can be performed in a manner such that network realizability is assured (at least from a theoretical viewpoint). However, any such transformation will be of practical utility only if it is easily interpreted and/or leads to a desirable physical structure.

Guillemin [8] has shown that a useful linear transformation is obtained by multiplying the rows and columns of a parameter matrix by suitable constants. In carrying out this transformation on a static capacitance matrix, symmetry requires that each operation be applied to both a row and its corresponding column.

Mathematically, the transformation is given by

$$\boldsymbol{C}' = \boldsymbol{n}_N \boldsymbol{C} \boldsymbol{n}_N \rightarrow \begin{array}{c} \\ n_1\rightarrow \\ n_2\rightarrow \\ \\ \vdots \\ n_N\rightarrow \end{array} \begin{array}{c} \begin{array}{cccc} n_1 \downarrow & n_2 \downarrow & \cdots & n_N \downarrow \end{array} \\ \left[\begin{array}{c|c|c|c} c_{11} & -c_{12} & 0 & \\ \hline -c_{12} & c_{22} & & \\ \hline 0 & & & \\ \hline & & & c_{NN} \end{array}\right] \end{array} \tag{5}$$

where $\boldsymbol{n}_N$ is a diagonal matrix with elements $n_1, n_2, \cdots, n_N$. The transformed capacitance matrix $\boldsymbol{C}'$ is obtained by pre- and post-multiplication of a given matrix $\boldsymbol{C}$ by the diagonal matrix $\boldsymbol{n}_N$. The right-hand portion of (5) indicates a convenient notation for use in applying the transformation to practical problems and serves to illustrate how each ith row and its corresponding column is multiplied by the same constant n_i.

To give a network interpretation to the capacitance matrix transformation of (5), consider the addition of ideal transformers of turns ratio n_i:1 to the $2N$-ports of the N-line network shown in Fig. 3(a). The resultant network is shown in Fig. 3(b). Physically, a new network has been formed with voltage and current variables related to those of the original network by

[1] This section is directed toward the definition and interpretation of capacitance matrix transformations. A more general discussion of equivalent network concepts can be found in Guillemin [8], pp. 141–176.

$$\begin{bmatrix} V_A' \\ \hline V_B' \end{bmatrix} = \left[\begin{array}{c|c} \boldsymbol{n}_N^{-1} & 0 \\ \hline 0 & \boldsymbol{n}_N^{-1} \end{array}\right] \begin{bmatrix} V_A \\ \hline V_B \end{bmatrix} \quad \text{and} \quad \begin{bmatrix} I_A' \\ \hline I_B' \end{bmatrix} = \left[\begin{array}{c|c} \boldsymbol{n}_N & 0 \\ \hline 0 & \boldsymbol{n}_N \end{array}\right] \begin{bmatrix} I_A \\ \hline I_B \end{bmatrix} \tag{6}$$

where $\boldsymbol{n}_N$ is a diagonal $N \times N$ matrix with elements $n_1, n_2, \cdots, n_N$, and $\boldsymbol{n}_N^{-1}$ is a diagonal $N \times N$ matrix with elements $1/n_1, 1/n_2, \cdots, 1/n_N$. Then from (1) and (6)

$$\begin{bmatrix} I_A' \\ \hline I_B' \end{bmatrix} = \frac{1}{\eta_0 S} \left[\begin{array}{c|c} \boldsymbol{n}_N & 0 \\ \hline 0 & \boldsymbol{n}_N \end{array}\right] \left[\begin{array}{c|c} \boldsymbol{C} & -\boldsymbol{C}\sqrt{1-S^2} \\ \hline -\boldsymbol{C}\sqrt{1-S^2} & \boldsymbol{C} \end{array}\right] \left[\begin{array}{c|c} \boldsymbol{n}_N & 0 \\ \hline 0 & \boldsymbol{n}_N \end{array}\right] \begin{bmatrix} V_A' \\ \hline V_B' \end{bmatrix} \tag{7}$$

where

$$\left[\begin{array}{c|c} \boldsymbol{n}_N^{-1} & 0 \\ \hline 0 & \boldsymbol{n}_N^{-1} \end{array}\right]^{-1} = \left[\begin{array}{c|c} \boldsymbol{n}_N & 0 \\ \hline 0 & \boldsymbol{n}_N \end{array}\right].$$

Thus

$$\begin{aligned} \begin{bmatrix} I_A' \\ \hline I_B' \end{bmatrix} &= \frac{1}{\eta_0 S} \left[\begin{array}{c|c} \boldsymbol{n}_N\boldsymbol{C}\boldsymbol{n}_N & -\boldsymbol{n}_N\boldsymbol{C}\boldsymbol{n}_N\sqrt{1-S^2} \\ \hline -\boldsymbol{n}_N\boldsymbol{C}\boldsymbol{n}_N\sqrt{1-S^2} & \boldsymbol{n}_N\boldsymbol{C}\boldsymbol{n}_N \end{array}\right] \begin{bmatrix} V_A' \\ \hline V_B' \end{bmatrix} \\ &\frac{1}{\eta_0 S} \left[\begin{array}{c|c} \boldsymbol{C}' & -\boldsymbol{C}'\sqrt{1-S^2} \\ \hline -\boldsymbol{C}'\sqrt{1-S^2} & \boldsymbol{C}' \end{array}\right] \begin{bmatrix} V_A' \\ \hline V_B' \end{bmatrix}. \end{aligned} \tag{8}$$

Referring to (8), the new matrix $\boldsymbol{C}' = \boldsymbol{n}_N\boldsymbol{C}\boldsymbol{n}_N$ is exactly that given by the capacitance matrix transformation of (5). However, the new matrix $\boldsymbol{C}'$ is also a matrix corresponding to a parallel line array and can be realized by simply changing the cross-sectional geometry from that of the original network as depicted in Fig. 3(c). The following statement summarizes the network and physical implications of the capacitance matrix transformation:

> given a parallel line array, transformation of the corresponding matrix $\boldsymbol{C}$ results in a matrix $\boldsymbol{C}'$ that corresponds to a new network identical to the original with ideal transformers of turns ratio n_i:1 added at both ends of each line. Physically, the new network can be realized by a change in cross-sectional geometry.

The factors n_i used in performing a capacitance matrix transformation can be chosen arbitrarily as long as they lead to a transformed capacitance matrix whose elements obey the restrictions given by (3).

The remaining question to be investigated is the following: under what conditions can the cross-sectional geometry be altered while a specified network response is held invariant? The answer becomes clear upon studying the diagrams of Fig. 3. If each of the $2N$-ports of the parallel line array of Fig. 3(a) is terminated in a passive admittance Y_i ($i=1 \cdots 2N$) then addition of ideal transformers [as in Fig. 3(b)] will affect only the network admittance level at any driven port. However, each terminating admittance Y_i can be transformed through the ideal transformers to yield primed terminating admittance $Y_i' = n_i^2 Y_i$. The original network and ideal transformers can then be replaced by a new network with a different cross-sectional geometry as described. The above statements are summarized as follows:

> the transmission response of a parallel line network with capacitance matrix $\boldsymbol{C}$ and line terminations Y_i is identical to that of a parallel line network with capacitance matrix $\boldsymbol{C}'$ and terminations $Y_i' = n_i^2 Y_i$, where the n_i are the constants utilized in transforming $\boldsymbol{C}$ into $\boldsymbol{C}'$.

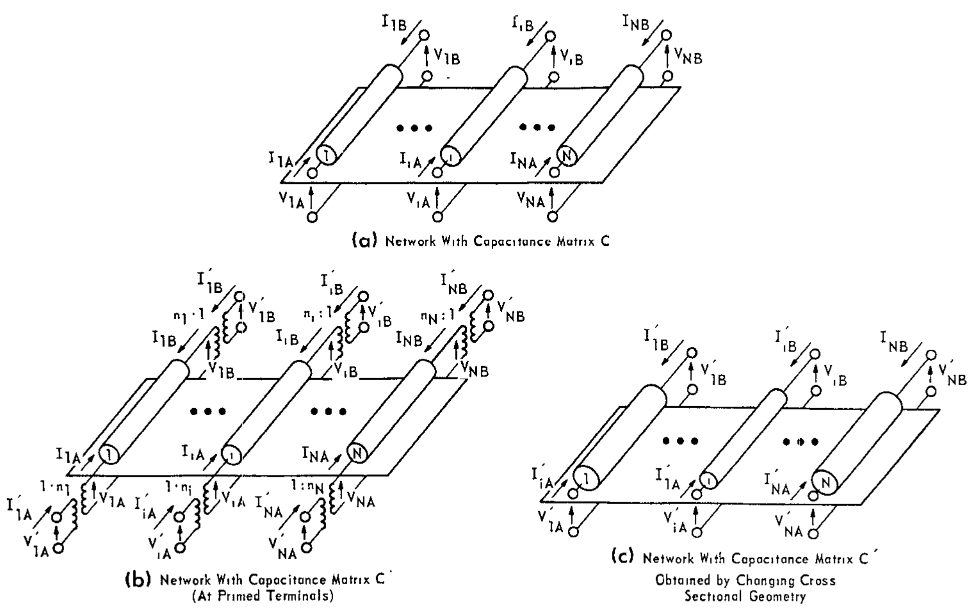

Fig. 3. Network and physical interpretation of the capacitance matrix transformation.

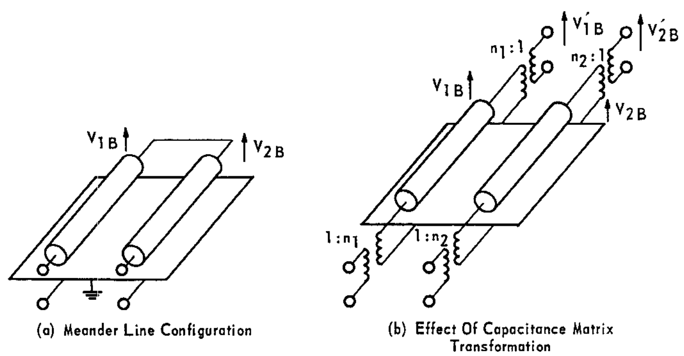

Fig. 4. Example illustrating inadmissible terminating conditions.

From the above statement, all complex terminating admittances, including opens and shorts, can be accommodated. It is emphasized that only terminations connected at the ports defined between the end of each line and the ground plane be considered in obtaining equivalent circuits by a change in cross-sectional geometry. An example of a network configuration for which an equivalent circuit cannot be realized by a change in cross-sectional geometry only is the familiar meander line shown in Fig. 4(a). Only two lines are shown for simplicity. Transformations of the capacitance matrix of the basic array introduce ideal transformers as shown in Fig. 4(b). As is readily seen, the original boundary condition that $V_{1B}=V_{2B}$ cannot be satisfied by making $V'_{1B}=V'_{2B}$ except when $n_1=n_2$. However, choosing $n_1=n_2$ is a trivial transformation that merely changes the impedance level of the entire network. The above example does not invalidate the use of the capacitance matrix transformation, but emphasizes that only under the specified terminating conditions can the transformation be interpreted as a simple change in cross-sectional geometry.

III. TEM Network Applications of Capacitance Matrix Transformations

A. Symmetric Directional Coupler Equivalent Circuits

As an example of some familiar equivalent circuits obtainable by application of the capacitance matrix transformation, consider the matched single-section four-port parallel line directional coupler shown in Fig. 5(a). The matched constraint requires that $Z_o=\sqrt{Z_{oe}Z_{oo}}$, where Z_{oe} and Z_{oo} are the even- and odd-mode impedances and Z_o is the characteristic impedance of the terminating lines [10]. The normalized [1] even- and odd-mode static capacitance values (c) are related to the even- and odd-mode impedances [10] by

$$Z_{oe}=\frac{\eta_o}{\sqrt{\epsilon_r}\cdot c_{oe}} \quad \text{and} \quad Z_{oo}=\frac{\eta_o}{\sqrt{\epsilon_r}\cdot c_{oo}}\,. \tag{9}$$

The corresponding self and mutual static capacitance values are then those given in Fig. 5(b). The circuit of Fig. 5(b) can be considered as a degenerate three-line network above a grounded plane in which the center line is coupled to both outer lines, but is decoupled from

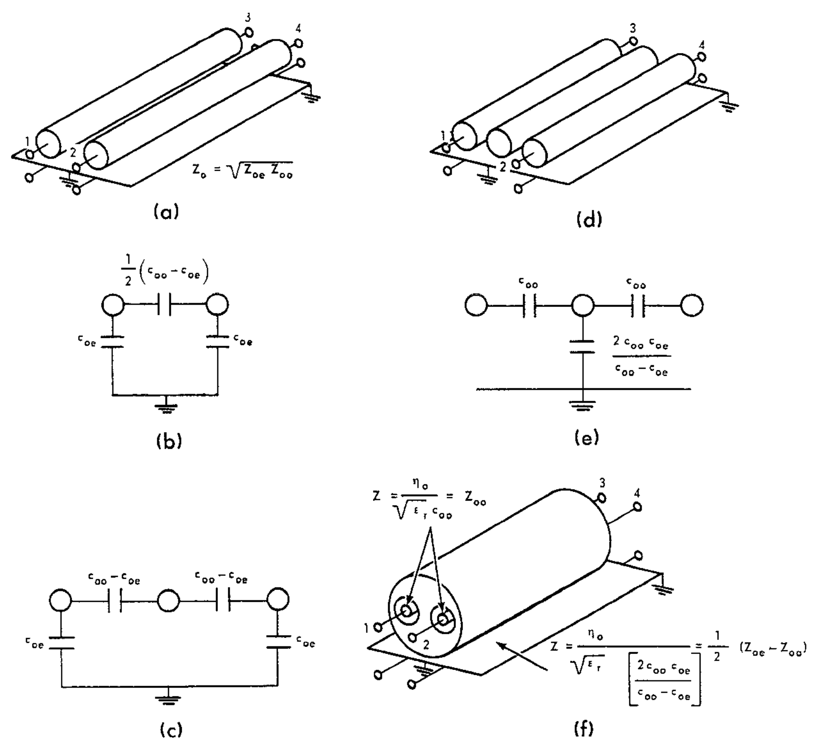

Fig. 5. Directional coupler equivalent circuits obtained by capacitance matrix transformations.

ground as shown in Fig. 5(c). The electrical performance of this network at ports one through four is identical to that of the two-line network of Fig. 5(b). The capacitance matrix for the network of Fig. 5(c) is

$$\begin{array}{cc} \left[\begin{array}{c|c|c} c_{oo} & -(c_{oo} - c_{oe}) & 0 \\ \hline -(c_{oo} - c_{oe}) & 2\,(c_{oo} - c_{oe}) & -(c_{oo} - c_{oe}) \\ \hline 0 & -(c_{oo} - c_{oe}) & c_{oo} \end{array}\right] & \begin{array}{c} \\ \leftarrow n. \\ \\ \end{array} \\ \begin{array}{ccc} \phantom{-(c_{oo} - c_{oe})} & \uparrow \\ & n & \end{array} & \end{array} \tag{10}$$

If the center row and column of this matrix is multiplied by an admissible constant n, the electrical performance at ports one through four is unchanged. The effect of a partial capacitance matrix transformation on the corresponding physical realization is shown in Fig. 5(d). A complete transformation results when the multiplying constant is chosen such that the outer lines are decoupled from the ground plane. This requires that the sum of elements in the first row or column of the capacitance matrix be zero. Therefore,

$$c_{oo} - n'(c_{oo} - c_{oe}) = 0 \quad \text{or} \quad n' = \frac{c_{oo}}{c_{oo} - c_{oe}} \cdot \tag{11}$$

The completely transformed network capacitance values are shown in Fig. 5(e) and a physical realization with appropriate impedance values is shown in Fig. 5(f). The transformed network is seen to be the re-entrant section described by Cohn [11]. The two-line directional coupler and the re-entrant coupled section are limiting cases of a more general three-line network. The two-line network results from a transformation that decouples the center line from the ground plane and the re-entrant section from a transformation that decouples the outer lines from the ground plane.

B. *Directional Couplers with Unequal Terminations*

The capacitance matrix transformation allows the simple design of directional couplers with unequal terminations. To demonstrate the technique, consider again the matched four-port directional coupler with coupling coefficient k shown in Fig. 6(a). The corresponding capacitance diagram is shown in Fig. 6(b) where the capacitance values are those given in Section III-A. The coupling coefficient is given by

$$k = \frac{\frac{1}{2}(c_{oo} - c_{oe})}{\frac{1}{2}(c_{oo} - c_{oe}) + c_{oe}} = \frac{c_{oo} - c_{oe}}{c_{oo} + c_{oe}} \cdot \tag{12}$$

The appropriate capacitance matrix is

$$\begin{array}{cc} \frac{1}{2}\left[\begin{array}{c|c} c_{oo} + c_{oe} & c_{oe} - c_{oo} \\ \hline c_{oe} - c_{oo} & c_{oo} + c_{oe} \end{array}\right] & \begin{array}{c} \\ \leftarrow n \end{array} \\ \begin{array}{cc} \phantom{c_{oo} + c_{oe}} & \uparrow \\ & n \end{array} & \end{array} \cdot \tag{13}$$

If an asymmetric transformation is performed by

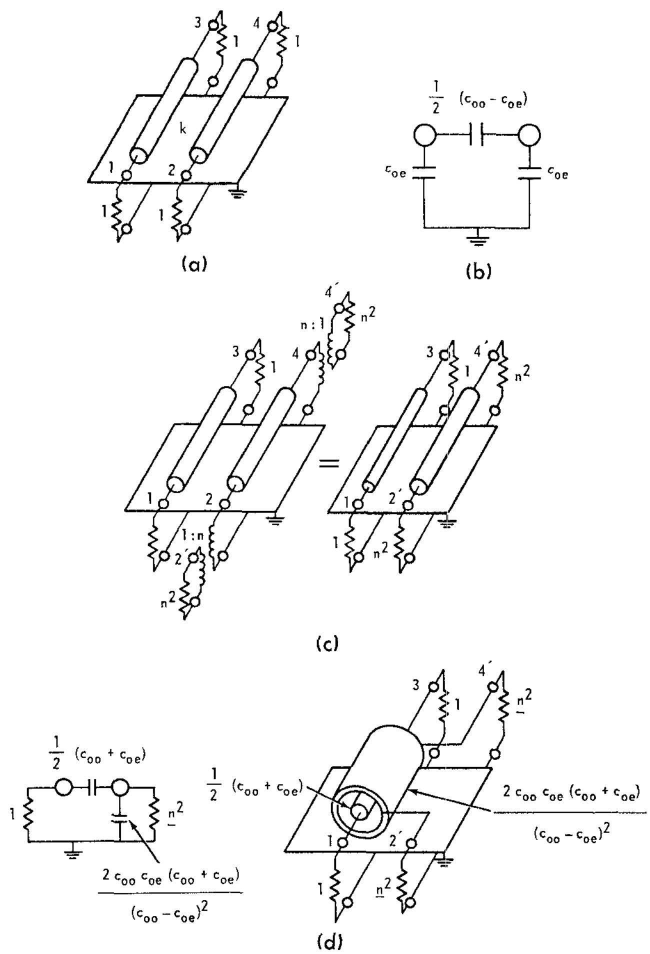

Fig. 6. Directional couplers with unequal terminations.

multiplying the second row and column by a factor n, a new capacitance matrix is obtained whose network realization is the original network with ideal transformers of turns ratio $n:1$ added to both ends of the second line. As described in Section II-B, if the unit terminating conductances are changed to a value of n^2, the original network with the ideal transformers added can be realized by a change in cross-sectional geometry while maintaining the transmission properties invariant. The network interpretation and a physical realization of a coupler corresponding to a partial transformation are shown in Fig. 6(c).

A complete transformation results if the self-capacitance from the first node is eliminated. From (13) this requires

$$n(c_{oo} - c_{oe}) = c_{oo} + c_{oe}$$

or

$$n = \frac{c_{oo} + c_{oe}}{c_{oo} - c_{oe}} = \frac{1}{k}. \tag{14}$$

A coaxial physical realization of a coupler corresponding to a complete capacitance matrix transformation is shown in Fig. 6(d) along with the appropriate capacitance network. From (14), the maximum termination ratio is seen to be dependent on coupling level, the ratio being given by

$$n_{\max}^2 = \frac{1}{k^2}. \tag{15}$$

As an example, a 3-dB coupler can yield at most a

$$\frac{1}{k^2} = \frac{1}{(0.707)^2} = 2:1$$

termination ratio. Also, as is evident from (15), the lower the coupling coefficient, the higher the possible termination ratio. The above procedure yields a transformation from a unity admittance value to a larger admittance value. Transformations from unity to smaller admittance values are obtained by changing the admittance level of the entire network and using the transformed line as reference.

C. Compact Filter-Transformers

In a previous paper [1], symmetric capacitance matrix transformations were utilized to obtain partial or entire coaxial realizations of interdigital filters. By applying an asymmetric transformation, compact coaxial interdigital filters that impedance transform in the passband, can be designed. These designs use the element value tables developed for the exact design of interdigital filters [12]. As with all impedance transforming devices, there are constraints imposed on the impedance ratio that can be achieved over a given bandwidth with a given tolerance and number of sections. These constraints have been investigated by straightforward application of the capacitance matrix transformation. The new network forms were found to be comparable in impedance transforming properties to quarter-wave stepped impedance designs using a like number of sections.

The normalized self and mutual static capacitance element values for interdigital filters with open-circuited terminating lines (OCTL) are given in Tables I–III for four, five, and six section designs, respectively.[2] Two ripple values, 0.01 dB (1.10 VSWR maximum) and 0.10 dB (1.36:1 VSWR maximum) are given. The tabulated element values can be used directly with available data, [1], [5], [6], and [13] to obtain physical dimensions for interdigital filters.

[2] More extensive element value tables including networks with short-circuited terminating lines (SCTL) are given in Reference [12]. The OCTL networks give a higher termination ratio for a specified number of sections and passband ripple than do the SCTL networks. The three tables given should be adequate for most filter-transformer requirements.

The following symbols are used in the tables presented:

N_f = number of filter sections (4, 5, or 6)
m = 3, number of L-C elements in basic prototype[3]
n = number of unit elements in basic prototype (1, 2, or 3)[3]
r = ripple value in dB (0.01 dB and 0.10 dB)
VSWR_M = maximum theoretical standing-wave ratio in the filter passband
% BW = percentage bandwidth
$F_H/F_L = (200+\%\ \mathrm{BW})/(200-\%\ \mathrm{BW})$ = ratio of high passband edge frequency to low passband edge frequency
R_S/R_L = maximum termination ratio determined by analysis. General formulas are given in each table for the specific configuration shown.

Concerning the filtering properties of the filter-transformers, the stop-band attenuation at transformed frequency Ω_A is given by [12], [14];

$$A = 10 \log_{10}\left[1 + \epsilon^2 \cosh^2\left(m \cosh^{-1} \frac{\Omega_c}{\Omega_A} + n \cosh^{-1} \frac{\sqrt{1+\Omega_c^2}}{\sqrt{1+\Omega_A^2}}\right)\right] \quad (16)$$

where

A = attenuation in dB
$\epsilon^2 = (10^{r/10} - 1)$
$\Omega_c = \tan \pi f_c/2f_0$
$\Omega_A = \tan \pi f_A/2f_0$
f_0 = frequency at which the lines are a quarter wavelength
f_c = cutoff frequency $= f_0[1 - \%\mathrm{BW}/200]$
f_A = frequency at which the attenuation is A dB

To demonstrate the use of the tables and the design techniques involved, a 3:1 bandwidth four-section filter transformer with 0.01 dB passband ripple will be described. The prototype self and mutual static capacitance values are obtained from Table I-A and are shown in Fig. 7(a). The capacitance matrix is:

$$\frac{1}{\sqrt{\epsilon_r}}\begin{bmatrix} 11.0 & -11.0 & 0 & 0 \\ -11.0 & 23.58 & -7.19 & 0 \\ 0 & -7.19 & 23.58 & -11.0 \\ 0 & 0 & -11.0 & 11.0 \end{bmatrix}. \quad (17)$$

The network of Fig. 7(a) is symmetric and is designed to work between equal terminating impedances. Unequal terminating impedances can be obtained by an asymmetrical transformation of the capacitance matrix, as discussed in Section II.

A desirable network configuration is one that contains only one shunt c in the corresponding capacitance network. This allows all other elements to be incorporated coaxially in the element represented by the single shunt c.

Referring to matrix (18), a single shunt c can be achieved by choosing n_1 and n_2 such that the desired network configuration, as shown in Fig. 7(b), is obtained.[4]

$$\frac{1}{\sqrt{\epsilon_r}}\begin{array}{c} \begin{bmatrix} 11.0 & -11.0 & 0 & 0 \\ -11.0 & 23.58 & -7.19n_1 & 0 \\ 0 & -7.19n_1 & 23.58n_1^2 & -11.0n_1n_2 \\ 0 & 0 & -11.0n_1n_2 & 11.0n_2^2 \end{bmatrix} \begin{array}{l} \\ \\ \leftarrow n_1 \\ \leftarrow n_2 \end{array} \\ \begin{array}{cccc} \qquad\qquad\qquad & \qquad\qquad & \uparrow & \uparrow \\ & & n_1 & n_2 \end{array} \end{array} . \quad (18)$$

This requires that:

$$-11.0 + 23.58 - 7.19n_1 = 0$$
$$11.0n_1n_2 = 11.0n_2^2$$
$$\therefore\ n_1 = n_2 = 1.75. \quad (19)$$

Then R_S/R_L = termination ratio $= n_2^2 = 3.06$.

Multiplication of the outer row and column of matrix (17) by $n_2 = 1.75$, as indicated in matrix (18), lowers the impedance level by $n_2^2 = 3.06$, and requires the use of a $1/n_2^2 = 0.327$ ohm load[5] to maintain a 0.01 dB ripple response in the passband. The transformed network thus acts as a 3.06:1 impedance transformer. The impedance ratio that can be achieved is limited by the choice of n_1 and n_2, which are constrained, as described in Section II. A higher impedance ratio can be achieved by applying another transformation such that the single shunt capacitor is connected to the fourth node. Referring to matrix (18), this requires that:

[3] The significance of m and n is described in detail in References [12] and [14].

[4] Note that the formulas for R_S/R_L given in each table allow the calculation of the achievable termination ratio for the configurations shown. Actual capacitance values are obtained as described in the design example.

[5] On a normalized 1-ohm basis.

$$-11.0 + 23.58 - 7.19n_1 = 0$$
$$-7.19n_1 + 23.58n_1^2 - 11.0n_1n_2 = 0. \tag{20}$$

Solving gives

$$n_1 = 1.75$$
$$n_2 = 3.09, \tag{21}$$

and results in a termination ratio of $n_2^2 = 9.6{:}1$. The corresponding capacitance network is shown in Fig. 7(c). Whereas the network of Fig. 7(c) is capable of providing a higher impedance ratio over a given band than the network of Fig. 7(b), all elements must be incorporated coaxially in the end element. This requires the end element to be large and results in a difficult connector problem. For this reason a network form such as that of Fig. 7(b) is often preferable. Furthermore, in some applications it is desirable to have not only a low impedance but also to have a region of high current density. This can be achieved by using a configuration such as that of Fig. 7(b).

Before describing experimental results, it is interesting to compare the transformer properties of the coaxial filter-transformer with those of quarter-wave stepped impedance lines. From Young's Tables [15], for 3:1 bandwidth, four quarter-wave sections give a maximum VSWR of 1.07:1 for a 3:1 impedance ratio and a maximum VSWR of 1.18:1 for a 10:1 impedance ratio. The partially transformed filter network [Fig. 7(b)] is comparable to the four-section quarter-wave stepped impedance design and the fully transformed network is superior to a stepped impedance design.

A trial transformer was constructed based on the capacitance network shown in Fig. 7(b). The corresponding S-plane equivalent circuit on a 50-ohm basis is shown in Fig. 8(a). The element values (C_1, Z, L, C_2) are directly related to the static capacitor values, as shown in (22). The corresponding impedance values on a 50-ohm basis for all-coaxial realization are:

$$\begin{aligned}
\frac{1}{C_1} &= Z_1 = \frac{\eta_0}{\sqrt{\epsilon_r}\, c_0} = \frac{376.7}{11.0} = 35.2 \text{ ohms} \\
Z &= Z_2 = \frac{\eta_0}{\sqrt{\epsilon_r}\, c_2} = \frac{376.7}{12.58} = 30.0 \text{ ohms} \\
L &= Z_3 = \frac{\eta_0}{\sqrt{\epsilon_r}\, c_3} = \frac{376.7}{35.8} = 14.6 \text{ ohms} \\
\frac{1}{C_2} &= Z_4 = \frac{\eta_0}{\sqrt{\epsilon_r}\, c_4} = \frac{376.7}{33.7} = 11.2 \text{ ohms}
\end{aligned} \tag{22}$$

where

$c_0 - c_4$ = static capacitance values shown in Fig. 7(b).

The corresponding diameter ratios are [13] (for teflon, $\sqrt{\epsilon_r} = 1.44$)

$$\begin{aligned}
d_{Z_1} &= 2.28_{\text{in teflon}} \\
d_{Z_2} &= 1.65_{\text{in air}} \\
d_{Z3} &= 1.27_{\text{in air}} \\
d_{Z4} &= 1.34_{\text{in teflon}}.
\end{aligned} \tag{23}$$

A schematic cross-sectional drawing showing the location of the various elements and appropriate impedances is shown in Fig. 8(b). Symbols have been added to important junction points in Figs. 8(a) and 8(b) to aid in visualizing the relationship between the prototype network and its physical realization. A detailed line drawing of the filter assembly, including dimensions, is given in Fig. 9.

The design center frequency chosen was 2.0 GHz. The line elements were arbitrarily shortened by 0.100 inch to compensate for end effects. Since a 50/3.06 = 16.3 ohm load was not available, a 50-ohm connector was attached to the low impedance end and tests were conducted by measuring the VSWR and insertion loss on a 50-ohm basis. The input impedance of a doubly terminated Chebyshev filter with small passband ripple is essentially real in its passband; therefore, a good indication of trial design performance can be obtained by measuring the input VSWR at the low impedance end. The VSWR value should be very nearly the transformer impedance ratio of 3.06:1. Again, because of the essentially real character of the input impedance, the performance that would have been achieved if a 16.3 ohm load had been available can be computed to good approximation by

$$\begin{aligned}
\text{VSWR}_{16.4\text{ ohm load}} &= \frac{\text{VSWR}_{50\text{ ohm load}}}{3.06}, \\
&\quad \text{when } \text{VSWR}_{50\text{ ohm load}} \geq 3.06 \\
\text{VSWR}_{16.4\text{ ohm load}} &= \frac{3.06}{\text{VSWR}_{50\text{ ohm load}}}, \\
&\quad \text{when } \text{VSWR}_{50\text{ ohm load}} \leq 3.06.
\end{aligned} \tag{24}$$

The measured and computed performance characteristics, together with theoretical values, are shown in Fig. 10. The experimental characteristics shown were achieved with the initial design—no alterations in dimensions were made. The performance is observed to be excellent in the initial design and indicates that transformers of the type described offer the possibility of achieving wideband impedance transforming networks in a very compact configuration. A photograph of the disassembled filter-transformer is shown in Fig. 11.

The filter-transformers described need not use an all-coaxial realization. Partial capacitance matrix transformations can be performed that allow coupled bar realizations to be employed, as described in [1]. Various geometric configurations can be investigated using the capacitance matrix transformation to achieve a desired configuration and/or more convenient line impedance values.

TABLE I

SELF AND MUTUAL STATIC CAPACITORS FOR CHEBYSHEV INTERDIGITAL FILTERS WITH OPEN-CIRCUITED TERMINATING LINES $m=3$, $n=1$, $N_f=4$ SECTIONS

A

r = 0.01 DB $VSWR_M$ = 1.10:1

% BW	$\sqrt{\epsilon_r}\, c_0$	$\sqrt{\epsilon_r}\, c_1$	$\sqrt{\epsilon_r}\, c_2$
30.0	.255E+01	.316E+02	.719E+01
35.0	.300E+01	.262E+02	.719E+01
40.0	.346E+01	.221E+02	.719E+01
45.0	.393E+01	.190E+02	.719E+01
50.0	.443E+01	.165E+02	.719E+01
55.0	.494E+01	.144E+02	.719E+01
60.0	.547E+01	.127E+02	.719E+01
65.0	.602E+01	.113E+02	.719E+01
70.0	.661E+01	.101E+02	.719E+01
75.0	.722E+01	.902E+01	.719E+01
80.0	.788E+01	.811E+01	.719E+01
85.0	.857E+01	.730E+01	.719E+01
90.0	.932E+01	.659E+01	.719E+01
95.0	.101E+02	.596E+01	.719E+01
100.0	.110E+02	.539E+01	.719E+01
110.0	.129E+02	.441E+01	.719E+01
120.0	.153E+02	.360E+01	.719E+01
130.0	.183E+02	.292E+01	.719E+01
140.0	.222E+02	.233E+01	.719E+01
150.0	.276E+02	.183E+01	.719E+01

B

r = 0.10 DB $VSWR_M$ = 1.36:1

% BW	$\sqrt{\epsilon_r}\, c_0$	$\sqrt{\epsilon_r}\, c_1$	$\sqrt{\epsilon_r}\, c_2$
30.0	.164E+01	.354E+02	.648E+01
35.0	.192E+01	.295E+02	.648E+01
40.0	.222E+01	.250E+02	.648E+01
45.0	.252E+01	.215E+02	.648E+01
50.0	.283E+01	.188E+02	.648E+01
55.0	.315E+01	.165E+02	.648E+01
60.0	.349E+01	.146E+02	.648E+01
65.0	.384E+01	.130E+02	.648E+01
70.0	.421E+01	.116E+02	.648E+01
75.0	.459E+01	.105E+02	.648E+01
80.0	.500E+01	.942E+01	.648E+01
85.0	.544E+01	.850E+01	.648E+01
90.0	.590E+01	.769E+01	.648E+01
95.0	.640E+01	.697E+01	.648E+01
100.0	.693E+01	.631E+01	.648E+01
110.0	.815E+01	.519E+01	.648E+01
120.0	.962E+01	.425E+01	.648E+01
130.0	.115E+02	.345E+01	.648E+01
140.0	.138E+02	.276E+01	.648E+01
150.0	.171E+02	.216E+01	.648E+01

$$\frac{F_H}{F_L} = \frac{200 + \%\,BW}{200 - \%\,BW}$$

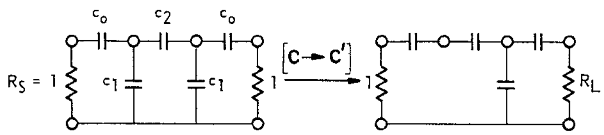

$$\frac{R_S}{R_L} = \left[1 + \frac{c_1}{c_2}\right]^2$$

TABLE II

SELF AND MUTUAL STATIC CAPACITORS FOR CHEBYSHEV INTERDIGITAL FILTERS WITH OPEN-CIRCUITED TERMINATING LINES $m=3$, $n=2$, $N_f=5$ SECTIONS

A

r = 0.01 DB $VSWR_M$ = 1.10:1

% BW	$\sqrt{\epsilon_r}\, c_0$	$\sqrt{\epsilon_r}\, c_1$	$\sqrt{\epsilon_r}\, c_2$	$\sqrt{\epsilon_r}\, c_3$
30.0	.240E+01	.350E+02	.688E+01	.293E+02
35.0	.282E+01	.291E+02	.688E+01	.235E+02
40.0	.326E+01	.246E+02	.689E+01	.193E+02
45.0	.371E+01	.212E+02	.690E+01	.160E+02
50.0	.417E+01	.184E+02	.691E+01	.134E+02
55.0	.465E+01	.162E+02	.692E+01	.113E+02
60.0	.515E+01	.143E+02	.693E+01	.960E+01
65.0	.567E+01	.127E+02	.694E+01	.819E+01
70.0	.622E+01	.113E+02	.695E+01	.701E+01
75.0	.681E+01	.101E+02	.697E+01	.601E+01
80.0	.742E+01	.910E+01	.698E+01	.515E+01
85.0	.808E+01	.820E+01	.699E+01	.442E+01
90.0	.879E+01	.739E+01	.701E+01	.379E+01
95.0	.955E+01	.667E+01	.702E+01	.325E+01
100.0	.104E+02	.602E+01	.703E+01	.278E+01
110.0	.123E+02	.491E+01	.706E+01	.201E+01
120.0	.145E+02	.398E+01	.708E+01	.143E+01
130.0	.174E+02	.320E+01	.710E+01	.994E+00
140.0	.212E+02	.254E+01	.713E+01	.665E+00
150.0	.265E+02	.196E+01	.714E+01	.423E+00

B

r = 0.10 DB $VSWR_M$ = 1.36:1

% BW	$\sqrt{\epsilon_r}\, c_0$	$\sqrt{\epsilon_r}\, c_1$	$\sqrt{\epsilon_r}\, c_2$	$\sqrt{\epsilon_r}\, c_3$
30.0	.158E+01	.376E+02	.629E+01	.322E+02
35.0	.186E+01	.313E+02	.630E+01	.261E+02
40.0	.214E+01	.266E+02	.630E+01	.215E+02
45.0	.243E+01	.229E+02	.630E+01	.180E+02
50.0	.274E+01	.200E+02	.631E+01	.152E+02
55.0	.305E+01	.176E+02	.631E+01	.129E+02
60.0	.337E+01	.156E+02	.632E+01	.111E+02
65.0	.371E+01	.139E+02	.632E+01	.955E+01
70.0	.407E+01	.124E+02	.633E+01	.825E+01
75.0	.444E+01	.112E+02	.634E+01	.714E+01
80.0	.484E+01	.101E+02	.634E+01	.618E+01
85.0	.526E+01	.910E+01	.635E+01	.536E+01
90.0	.571E+01	.823E+01	.636E+01	.464E+01
95.0	.619E+01	.745E+01	.636E+01	.402E+01
100.0	.671E+01	.675E+01	.637E+01	.347E+01
110.0	.789E+01	.553E+01	.639E+01	.257E+01
120.0	.933E+01	.451E+01	.640E+01	.187E+01
130.0	.111E+02	.365E+01	.642E+01	.132E+01
140.0	.135E+02	.291E+01	.643E+01	.907E+00
150.0	.167E+02	.227E+01	.644E+01	.589E+00

$$\frac{F_H}{F_L} = \frac{200 + \%\,BW}{200 - \%\,BW}$$

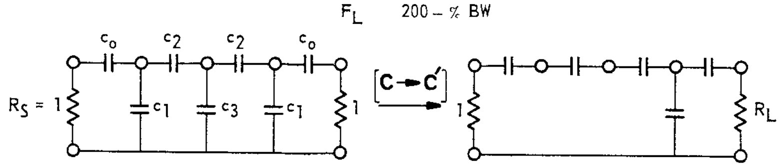

$$\frac{R_S}{R_L} = \left[\left(1 + \frac{c_1}{c_2}\right)\left(2 + \frac{c_3}{c_2}\right) - 1\right]^2$$

TABLE III

SELF AND MUTUAL STATIC CAPACITORS FOR CHEBYSHEV INTERDIGITAL FILTERS WITH OPEN-CIRCUITED TERMINATING LINES $m=3$, $n=3$, $N_f=6$ SECTIONS

A

$r = 0.01$ DB $\quad$ $VSWR_M = 1.10:1$

% BW	$\sqrt{\epsilon_r}\, c_0$	$\sqrt{\epsilon_r}\, c_1$	$\sqrt{\epsilon_r}\, c_2$	$\sqrt{\epsilon_r}\, c_3$	$\sqrt{\epsilon_r}\, c_4$
30.0	.232E+01	.368E+02	.678E+01	.314E+02	.640E+01
35.0	.273E+01	.306E+02	.679E+01	.253E+02	.641E+01
40.0	.315E+01	.260E+02	.679E+01	.208E+02	.642E+01
45.0	.358E+01	.224E+02	.680E+01	.174E+02	.644E+01
50.0	.403E+01	.195E+02	.681E+01	.146E+02	.645E+01
55.0	.449E+01	.171E+02	.682E+01	.124E+02	.647E+01
60.0	.497E+01	.151E+02	.683E+01	.106E+02	.649E+01
65.0	.548E+01	.135E+02	.684E+01	.906E+01	.651E+01
70.0	.601E+01	.120E+02	.685E+01	.778E+01	.654E+01
75.0	.656E+01	.108E+02	.687E+01	.670E+01	.656E+01
80.0	.716E+01	.971E+01	.688E+01	.577E+01	.659E+01
85.0	.779E+01	.875E+01	.690E+01	.497E+01	.662E+01
90.0	.847E+01	.789E+01	.691E+01	.427E+01	.664E+01
95.0	.920E+01	.713E+01	.693E+01	.367E+01	.667E+01
100.0	.999E+01	.644E+01	.694E+01	.314E+01	.671E+01
110.0	.118E+02	.525E+01	.698E+01	.229E+01	.677E+01
120.0	.140E+02	.426E+01	.701E+01	.163E+01	.684E+01
130.0	.168E+02	.342E+01	.704E+01	.113E+01	.690E+01
140.0	.205E+02	.270E+01	.708E+01	.751E+00	.697E+01
150.0	.257E+02	.208E+01	.711E+01	.473E+00	.703E+01

B

$r = 0.10$ DB $\quad$ $VSWR_M = 1.36:1$

% BW	$\sqrt{\epsilon_r}\, c_0$	$\sqrt{\epsilon_r}\, c_1$	$\sqrt{\epsilon_r}\, c_2$	$\sqrt{\epsilon_r}\, c_3$	$\sqrt{\epsilon_r}\, c_4$
30.0	.155E+01	.386E+02	.624E+01	.334E+02	.601E+01
35.0	.182E+01	.322E+02	.624E+01	.271E+02	.601E+01
40.0	.210E+01	.274E+02	.624E+01	.225E+02	.602E+01
45.0	.239E+01	.236E+02	.625E+01	.188E+02	.603E+01
50.0	.268E+01	.206E+02	.625E+01	.160E+02	.604E+01
55.0	.299E+01	.182E+02	.626E+01	.136E+02	.605E+01
60.0	.331E+01	.161E+02	.626E+01	.117E+02	.606E+01
65.0	.364E+01	.144E+02	.627E+01	.101E+02	.607E+01
70.0	.399E+01	.129E+02	.627E+01	.874E+01	.608E+01
75.0	.435E+01	.116E+02	.628E+01	.758E+01	.609E+01
80.0	.474E+01	.104E+02	.629E+01	.658E+01	.610E+01
85.0	.515E+01	.943E+01	.630E+01	.571E+01	.612E+01
90.0	.559E+01	.854E+01	.630E+01	.496E+01	.613E+01
95.0	.606E+01	.773E+01	.631E+01	.430E+01	.615E+01
100.0	.657E+01	.701E+01	.632E+01	.372E+01	.617E+01
110.0	.773E+01	.575E+01	.634E+01	.276E+01	.620E+01
120.0	.914E+01	.469E+01	.636E+01	.201E+01	.624E+01
130.0	.109E+02	.380E+01	.638E+01	.143E+01	.628E+01
140.0	.132E+02	.302E+01	.640E+01	.975E+00	.632E+01
150.0	.164E+02	.235E+01	.642E+01	.631E+00	.636E+01

$$\frac{F_H}{F_L} = \frac{200 + \%\,BW}{200 - \%\,BW}$$

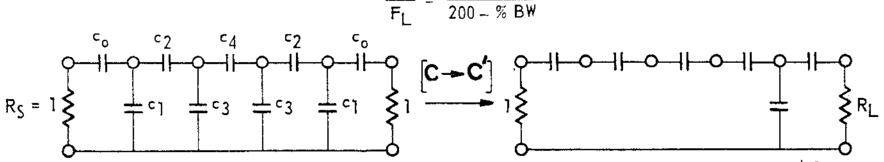

$$\frac{R_S}{R_L} = n_1^2 n_2^2 n_3^2 \quad \text{WHERE}$$

$$n_1 = 1 + \frac{c_1}{c_2} \qquad n_3 = 1 + \frac{c_3 + c_4}{c_2} - \frac{c_4}{c_2 n_2}$$

$$n_2 = 1 + \frac{c_2 + c_3}{c_4} - \frac{c_2}{c_4 n_1}$$

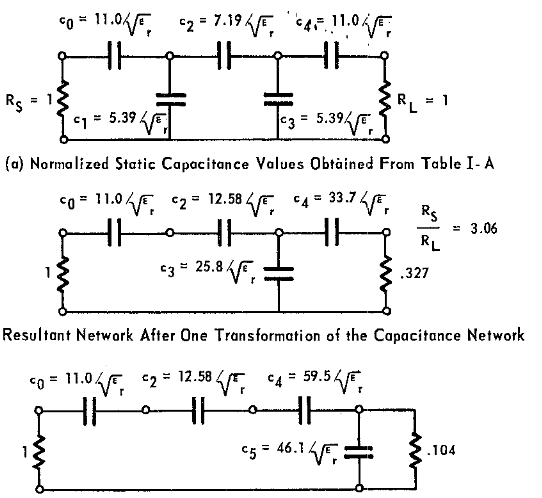

(a) Normalized Static Capacitance Values Obtained From Table I-A

(b) Resultant Network After One Transformation of the Capacitance Network

(c) Network with Largest Possible Transformer Ratio

Fig. 7. Coaxial filter-transformer design.

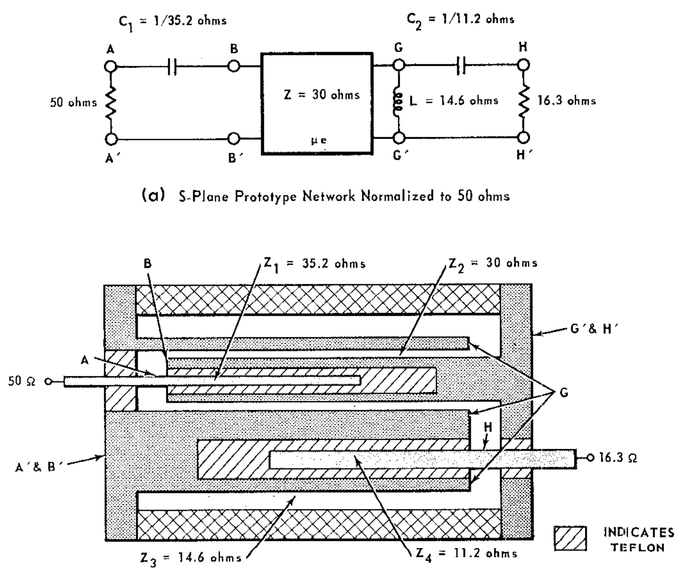

(a) S-Plane Prototype Network Normalized to 50 ohms

(b) Schematic Cross-Sectional Drawing

Fig. 8. Coaxial filter-transformer schematic diagram.

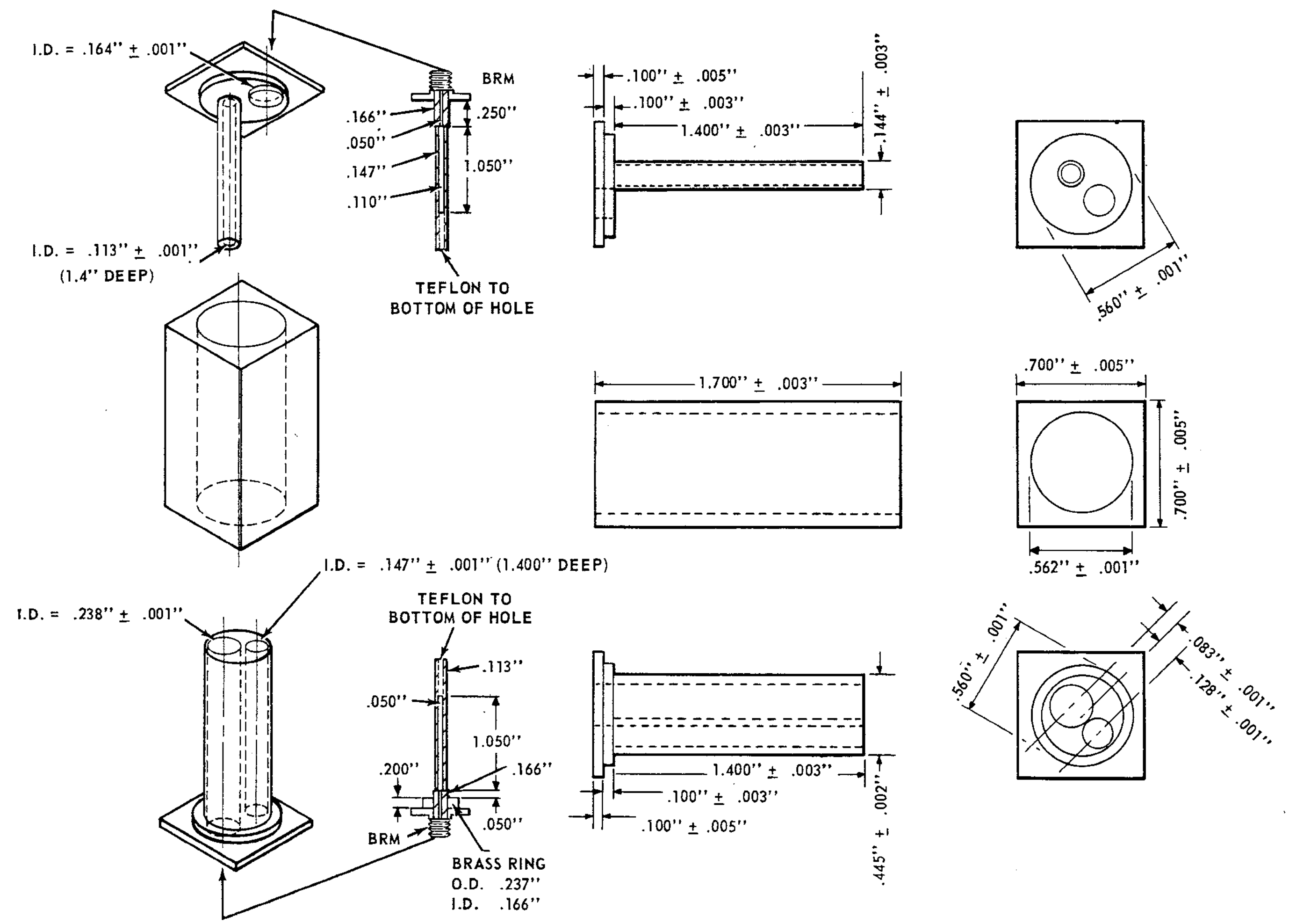

Fig. 9. Assembly drawing of 3:1 bandwidth filter-transformer.

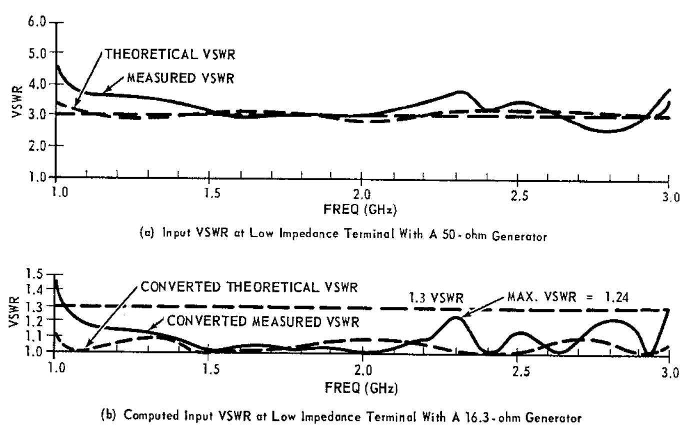

Fig. 10. Theoretical and measured performance of 3:1 bandwidth filter-transformer.

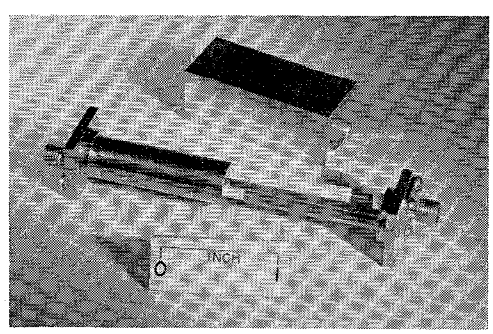

Fig. 11. Four-section coaxial filter-transformer.

Conclusions

The description of TEM propagation on an array of parallel coupled lines in terms of the static capacitance matrix allows a unified treatment of many heretofore seemingly unrelated network configurations. The use of the capacitance matrix transformation provides a simple method, devoid of complicated mathematics, for investigating possible equivalent circuit structures and obtaining new network forms. Furthermore, the techniques described provide considerable physical insight into the meaning of equivalent TEM networks and should be a very useful tool, both computationally and conceptually, to the network designer.

References

[1] R. J. Wenzel, "Exact theory of interdigital band-pass filters and related coupled structures," *IEEE Trans. on Microwave Theory and Techniques*, vol. MTT-13, pp. 559–575, September 1965.

[2] S. O. Rice, "Steady-state solutions of transmission line equations," *Bell Sys. Tech. J.*, vol. 20, pp. 131–178, April 1941.

[3] D. C. Youla, "An introduction to coupled-line network theory," MRI, Polytechnic Institute of Brooklyn, Brooklyn, N. Y., Rept. 960–961, 1961.

[4] E. Ott, "A network approach to the design of multiline 2*N*-port directional couplers," Polytechnic Institute of Brooklyn, Brooklyn, N. Y., Rept. PIBMRI-1236-64; Air Research Development Command, Rome Air Development Center, Griffiss AFB, Rome, N. Y., Contract AF 30(602)-2868, Tech. Rept. RADC-TR-65-41, April 1965.

[5] W. J. Getsinger, "Coupled rectangular bars between parallel plates," *IRE Trans. on Microwave Theory and Techniques*, vol. MTT-10, pp. 65–72, January 1962.

[6] E. G. Cristal, "Coupled circulator cylindrical rods between parallel ground planes," *IEEE Trans. on Microwave Theory and Techniques*, vol. MTT-12, pp. 428–439, July 1964.

[7] R. W. Beatty and D. M. Kerns, "Relationships between different kinds of network parameters, not assuming reciprocity or equality of the waveguide or transmission line characteristic impedances," *Proc. IEEE* (*Correspondence*), vol. 52, p. 84, January 1964.

[8] E. A. Guillemin, *Synthesis of Passive Networks*. New York: Wiley, 1957.

[9] R. M. Fano, L. J. Chu, and R. B. Adler, *Electromagnetic Fields, Energy and Forces*. New York: Wiley, 1960.

[10] E. M. T. Jones and J. T. Bolljahn, "Coupled-strip-transmission-line filters and directional couplers," *IRE Trans. on Microwave Theory and Techniques*, vol. MTT-4, pp. 75–81, April 1956.

[11] S. B. Cohn, "The re-entrant cross section and wide-band 3-dB hybrid couplers," *IEEE Trans. on Microwave Theory and Techniques*, vol. MTT-11, pp. 254–258, July 1963.

[12] R. J. Wenzel and M. C. Horton, "Exact design techniques for microwave TEM filters," Final Rept., U. S. Army Electronics Lab., Fort Monmouth, N. J., 00399(E), Bendix Research Labs., Southfield, Mich., April 1965.

[13] *The Microwave Engineers Handbook and Buyer's Guide*. Brookline, Mass.: Horizon House-Microwave, Inc., 1966, p. 91.

[14] M. C. Horton and R. J. Wenzel, "General theory and design of optimum quarter-wave TEM filters," *IEEE Trans. on Microwave Theory and Techniques*, vol. MTT-13, pp. 316–327, May 1965.

[15] L. Young, "Tables for cascaded homogeneous quarter-wave transformers," *IRE Trans. on Microwave Theory and Techniques*, vol. MTT-9, pp. 233–237, April 1959.

The Design and Construction of Broadband, High-Directivity, 90-Degree Couplers Using Nonuniform Line Techniques

C. P. TRESSELT, MEMBER, IEEE

Abstract—**It is possible, at present, to obtain multioctave bandwidth in symmetrical couplers that employ cascaded quarter-wavelength sections of uniformly coupled line. However, the physical junctions between the various sections contribute reactive discontinuities, which significantly degrade coupler directivity. This paper describes a coupler design employing a continuously tapered coupling coefficient that helps to circumvent the directivity problem.**

Two classes of couplers have been investigated, including one which provides optimum equal-ripple performance. Synthesis has been performed with the aid of both digital and Fourier integral computers. Somewhat tighter center coupling is required in the tapered design to produce bandwidth-mean-coupling-level performance comparable to stepped-coupling design.

Experimental data is presented on several models constructed in three-layer polyolefin stripline.

Manuscript received June 29, 1966; revised August 8, 1966.

The author is with The Bendix Corporation, Research Laboratories Division, Southfield, Mich.

I. Introduction

It is possible to obtain multioctave bandwidth from a single coupler that employs several cascaded quarter-wavelength sections of uniformly coupled line. The use of a symmetric structure guarantees 90° relative phase lead of the coupled port with respect to the transmitted port at all frequencies. Cristal and Young [1] present tables of coupling coefficients required to produce equal-ripple response for the third- through ninth-order designs, and include a comprehensive bibliography covering the historic development of this form of coupler. Tight coupling normally is required in at least one of the sections of a broadband design. This condition has been alleviated to some extent by the application of tandem interconnection [2].